Protein Nanowires

DOI: 10.1002/ange.201300692

Construction of Protein Nanowires through Cucurbit[8]uril-based Highly Specific Host–Guest Interactions: An Approach to the Assembly of Functional Proteins**

*Chunxi Hou, Jiaxi Li, Linlu Zhao, Wei Zhang, Quan Luo, Zeyuan Dong, Jiayun Xu, and Junqiu Liu**

Protein nanostructures are of great interest in the field of bionics, owing not only to their biocompatible and biodegradable properties, but also to their high structural durability, which facilitates recycling. Some creative strategies have been developed to construct protein nanostructures based on molecular recognition, such as symmetry, metal ion induction, or supramolecular interactions.[1] Some protein nanostructures, such as artificial protein nanowires,[1a] protein rings,[1b] and protein spheres,[1c] have been created by these strategies and applied in catalysis, tissue imaging, diagnostics, and therapeutic treatments. Among them, host–guest supramolecular interactions have provided desirable driving forces in a reversible and bioorthogonal manner. Although host–guest interactions have been successfully developed using protein–ligand interactions, such as biotin–streptavidin,[2a,b] dihydrofolate reductase–methotrexate,[2c] and lectin concanavalin A–mannopyranoside,[2d] the construction of functional protein nanostructures by small molecule host–guest interactions has rarely been explored.

Cucurbit[*n*]uril is a series of robust macrocyclic hosts (CB[*n*]; $n = 5$–8, 10).[3] Owing to the great guest-binding ability of CB in aqueous media, CB homologues play a major role in the design of supramolecular nanostructures.[3a] Supramolecular structures ranging from oligomers to 3D structures have been successfully constructed by CB-based host–guest interactions. For example, Kim and co-workers have developed molecular necklaces through CB[8]-mediated interactions with a methylene-bridged naphthalene–dipyridyliumylethylene guest.[4a] Scherman and co-workers have reported a series of supramolecular hydrogels and microcapsules comprised of a strong, reversible CB[8]-based 1:1:1 ternary binding motif, typically with methyl viologen as the first guest and naphthoxy derivatives as the second guest.[4b,c] Furthermore, Zhang and co-workers have constructed supramolecular polymers formed by CB[8] and 1-(anthracen-2-ylmethyl)pyridinium bromide,[4d,e] and prepared CB[8]-adhered multilayer protein membranes.

Although CBs have been successfully used to bind many kinds of guest molecules, their recognition of amino acids and peptides plays a major role in the construction of biofunctional nanostructures. Host cucurbit[8]uril has been previously shown to be able to form complexes with special peptide sequences in a 1:2 ratio with Trp-Gly-Gly (WGG) or Phe-Gly-Gly (FGG), and with binding constants of up to 10^9–$10^{11}\,\text{M}^{-2}$.[5] Owing to strong binding affinity and selectivity, CB[8] functions as a powerful adhesive to effectively connect the guests. Protein dimerization has been achieved by CB[8] binding to FGG-tags on the N-termini of mYFP and mCFP.[5b,c] Inspired by these investigations, we wondered whether protein nanostructures can be assembled through this host–guest interaction. Herein, we report that protein nanowires are successfully assembled by CB[8]-based highly specific supramolecular interactions with tripeptide FGG fused with the N-termini of dimeric glutathione S-transferase (GST). To further construct the functional protein nanowires, the active site of selenoenzyme glutathione peroxidase (GPx) was introduced into GST tagged with FGG by genetic engineering with the aid of enzyme simulation. Utilizing this strategy, we constructed highly active protein nanowires with GPx-like activity. We further demonstrate that the enzyme-functionalized protein nanowires exhibit excellent antioxidative activity.

We chose the GST dimer as our model protein because His-tagged GST has been reported to have the potential to form nanowires by metal-ion induction.[6] For constructing GST nanowires (Figure 1), two FGG tags were fused with the N-termini of a GST homodimer. The FGG arms protrude from the asymmetric N-termini of the homodimer in an opposite orientation, which facilitates the induction of supramolecular interactions with host molecules. A two-way connector with strict selectivity and binding force was generated through the interactions of two FGG-tags and CB[8], thus allowing the C2-symmetric GST dimer to assemble into a GST homotetramer and further nanowires in the symmetric axis orientation.

The special recognition of FGG by CB[8] is the key step in constructing protein nanowires. The specific binding between FGG-GST and CB[8] was investigated by isothermal titration calorimetry (ITC; Figure 2a). The data best fit to a 2:1 homodimeric binding model, which yields exothermic interaction enthalpies of $1.32 \times 10^4\,\text{cal mol}^{-1}$ at 25 °C, which is in good agreement with that of protein dimerization induced by

[*] Dr. C. X. Hou, J. X. Li, L. L. Zhao, Dr. W. Zhang, Dr. Q. Luo, Dr. Z. Y. Dong, J. Y. Xu, Prof. Dr. J. Q. Liu
State Key Laboratory of Supramolecular Structure and Materials
College of Chemistry, Jilin University
2699 Qianjin Road, Changchun 130012 (China)
E-mail: junqiuliu@jlu.edu.cn

[**] We acknowledge financial support from the Natural Science Foundation of China (21234004, 91027023, 21221063, 21004028) and the 111 project (B06009).

Supporting information for this article is available on the WWW under http://dx.doi.org/10.1002/anie.201300692.

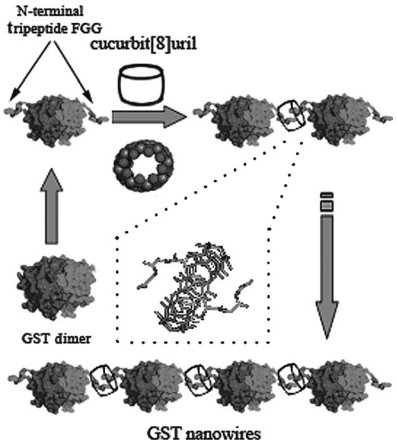

Figure 1. Formation of protein nanowires by CB[8]-based host–guest interactions. Natural GST is a C2-symmetric dimeric protein with a solvent-exposed N-terminus, onto which tripeptide FGG was appended. Nanowires from the C2-symmetric GST dimer can be formed from host–guest interactions of CB[8] and the N-terminal FGG of GST.

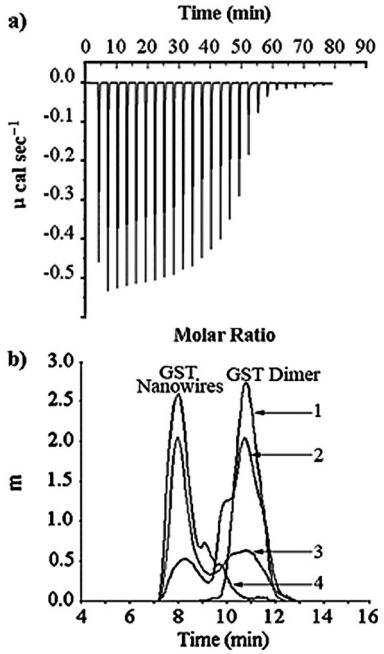

Figure 2. a) Isothermal titration calorimetry of the titration of GSH (75 μM) into FGG-GST (5 μM) at 25 °C. b) SEC of mixtures of FGG-GST (6 μM) and various concentrations of cucurbit[8]uril (0, 1.5, 3, and 6 μM for plots 1 to 4, respectively).

CB[8].[5b] Furthermore, ITC data demonstrated that CB[8] forms a complex with FGG-GST. The ternary formation constant of this CB[8]—$(FGG\text{-}GST)_2$ complex was found to be $2.9\times10^{12}\ M^{-2}$, which indicates a high affinity between FGG-GST and CB[8]. The above data showed that the FGG tag at the N-terminal of GST confers the strong binding affinity between FGG-GST and CB[8]. The complex formed by CB[8] with FGG-GST was further examined by size exclusion HPLC (SEC; Figure 2b). The addition of CB[8] to a FGG-GST solution resulted in a new peak at a retention time of 8.1 min, which indicates the presence of large FGG-GST assemblies. The ratio of CB[8]/FGG-GST was increased from 0 to 1:4 to 1:2, which led to an increased peak intensity at 8.1 min and a reduced peak intensity at 11 min. The data indicates an increased content of FGG-GST assemblies and a reduced content of dimeric FGG-GST. When the ratio of CB[8]/FGG-GST was increased to more than 1:1, all of the FGG-GST was assembled by CB[8] induction, as indicated by the disappearance of the peak of dimeric FGG-GST. Together, the data show that the interactions of CB[8] with FGG-GST are specific and that CB[8] and FGG-GST can form large and stable assemblies.

To investigate the morphology and the structure of CB[8]-induced FGG-GST nanostructures, we performed tapping-mode atomic force microscopy (AFM). As shown in Figure 3, the addition of CB[8] into a solution of FGG-GST generated FGG-GST nanowires, which indicates that there is a cooperative effect to form ordered aggregates. Specifically, when 0.25 equiv of CB[8] was added into a FGG-GST solution, long nanowires with lengths of up to 128 nm appeared (Figure 3a). The nanowires were (4.8 ± 0.3) nm in height, which is in agreement with the theoretical value of naturally occurring GST (5 nm). Moreover, the sphere-like FGG-GST particles were apparently divided by spacers, revealing that the FGG-GST dimers were bridged and assembled by the specific interactions between CB[8] and GST tagged with FGG (Figure 3a,c). When the amount of CB[8] was increased to

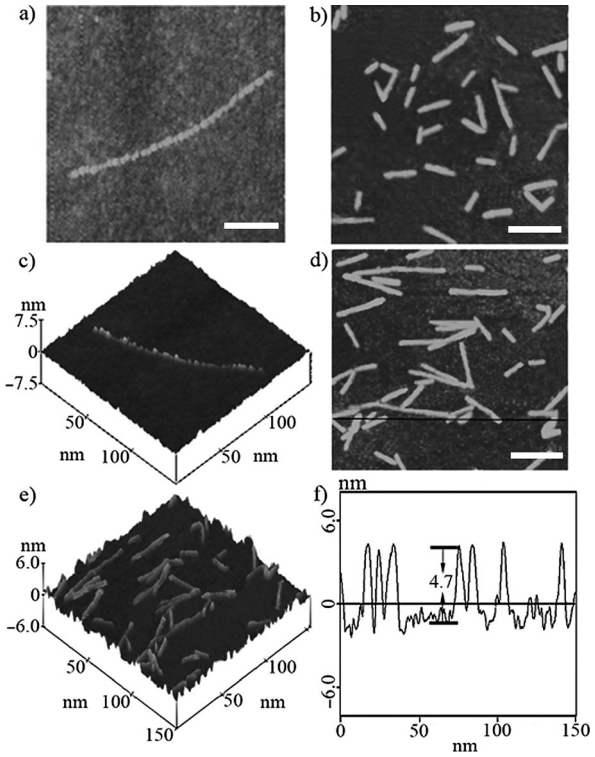

Figure 3. AFM images of FGG-GST nanowires and Se-FGG-GST (Y6C) nanowires induced by CB[8]. a) Single nanowire (CB[8]/FGG-GST = 1:4). b) Nanowires (CB[8]/FGG-GST = 1:2). c) An enlarged image of (a). d) Nanowires (CB[8]/Se-FGG-GST (Y6C) = 1:2). e) An enlarged image of (d). f) The height profile along the black line in (d). Scale bars in (a), (b), and (d) are 30 nm.

0.5 equiv in the system, more nanowire-like assemblies were formed, indicating that CB[8] acted as an efficient inducer (Figure 3b).

After the self-assembled protein nanostructure was successfully constructed, we wondered whether we could build up functional protein nanowires with this method. Recently, our group has reported the creation of artificial antioxidative glutathione peroxidase (GPx) through chemical and genetic-engineering strategies.[7] The GST enzyme has been shown to be an excellent scaffold to which a GPx catalytic center can be incorporated. Based on previous enzyme simulation strategies,[7,8] we designed a new GPx mimic based on *Schistosoma japonicum* GST, which exhibits high catalytic effectiveness (Figure 4).

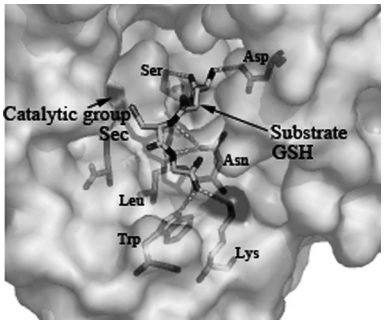

Figure 4. Computer simulation for the conversion of GST into a GPx mimic. Selenocysteine, the catalytic group of GPx, was assigned at site 6 of GST and was installed in Se-FGG-GST (Y6C) by cysteine auxotrophic expression system. Catalytic selenocysteine and substrate GSH are indicated by arrows, and important amino acids involved in catalysis and binding are exhibited.

Although both GST and GPx have a similar catalytic site with high recognition for substrate GSH, the catalytic group of GST involves a tyrosine or serine, whereas GPx uses selenocysteine as a catalytic group.[7] Computer-aided simulations indicate that the substitution of a catalytic tyrosine moiety with selenocysteine could be an efficient way to install a GPx function. Thus, we constructed functional building blocks by incorporating catalytic selenocysteine into the substrate-binding pocket of FGG-GST (Supporting Information, Schemes S1 and S2).

We chose a cysteine auxotrophic expression system to produce GPx mimic Se-FGG-GST (Y6C). Se-FGG-GST (Y6C) was purified by anion exchange chromatography and characterized by SDS-PAGE, MALDI-TOF and CD spectra (Figures S1–S4). The GPx activities were measured by a previously described coupled enzymatic method.[7a] As shown in Table 1, GST and FGG-GST did not exhibit GPx activities, but Se-FGG-GST (Y6C) had an activity of 1935.5 $\mu mol\,min^{-1}\,\mu mol^{-1}$, which indicates that both GPx and GST have a similarly highly conserved catalytic domain, and the selenocysteine was successfully incorporated into the substrate binding pocket. Se-FGG-GST (Y6C) also exhibited GPx activity using substrate cumene peroxide (237.4 $\mu mol\,min^{-1}\,\mu mol^{-1}$). Selenium content of Se-FGG-GST (Y6C) was determined to be 2.02 (one selenium per monomer), thus supporting the successful incorporation of selenium into Se-FGG-GST (Y6C). The activity of Se-FGG-GST was 262-fold higher than that of the GPx mimic 2-SeCD.[7c] Although the activity of Se-FGG-GST was not as high as native GPx species, such as rabbit liver GPx (5780 U),[7a] it is the best among the other GPX mimics (Figure S8).

Table 1: Activities of Se-FGG-GST (Y6C) and other GPx mimics.

Catalyst	Activity[a] [$\mu mol\,min^{-1}\,\mu mol^{-1}$]	Selenium [$\mu mol\,\mu mol^{-1}$]
GST[b]	n.d.	0
FGG-GST[c]	n.d.	0
Se-FGG-GST(Y6C)[d]	1935.5 ± 5.3	2.02
2-SeCD[e]	7.40	2.0
ebselen[f]	1.02	0.96
rabbit liver Gpx	5780	4.00

[a] The activity is defined as the amount of the enzyme that catalyzes the turnover of 1 μmol of NADPH per min. [b] Wild-type GST monomer has four intrinsic cysteines. The substrate in all cases is H_2O_2. [c] FGG-GST monomer is a cysteine-free mutant. [d] After auxotrophic expression, the Se-FGG-GST (Y6C) monomer has single selenocysteine at site 6. [e] Based on Ref. [7c]. [f] Based on Ref. [8a]. n.d. = not determined.

The Se-FGG-GST nanowires was generated by CB[8] induction of the Se-FGG-GST (Y6C) assembly using the same procedure as for FGG-GST nanowires. The morphology of Se-FGG-GST (Y6C) assemblies was investigated by tapping-mode AFM. Under the same conditions, similar nanowires were observed (Figure 3d,e). The height of the nanowires was (4.7 ± 0.3) nm, which is in agreement with the intrinsic height of natural GST (Figure 3f). The results demonstrated that selenium incorporation and genetic engineering did not affect the formation of nanowires. Furthermore, Se-FGG-GST (Y6C) nanowires exhibited significant storage stability compared with Se-FGG-GST (Y6C) monomers (Figure S9).

To ask whether the Se-FGG-GST (Y6C) nanowires have antioxidative capacities, we performed an assay of mitochondria oxidative stress.[6d,e] The slope of absorbance at A520 was decreased by adding GPx-functionalized Se-FGG-GST (Y6C) nanowires to the reaction mixture, which indicates that the integrity of mitochondria was protected (Figure S10). We also studied the production of the final oxidative product, malondialdehyde (MDA), in a lipid peroxidation reaction. Se-FGG-GST (Y6C) nanowires were more effective than unassembled Se-FGG-GST (Y6C) (Figure 5). Specifically, an average 20% increase in inhibition was observed at various concentrations of Se-FGG-GST (Y6C) nanowires compared to Se-FGG-GST (Y6C) monomers. Notably, the MDA content dropped from 93.5% to 68.2% in the presence of 10 nM Se-FGG-GST (Y6C) nanowires, which suggests that they are more effective for the inhibition of MDA production than Se-FGG-GST (Y6C) monomers. These results indicated that the Se-FGG-GST (Y6C) nanowires are attractive stable biomaterials with antioxidant properties that show promise for applications in biosensors and biomedicine.

In conclusion, we have constructed antioxidative protein nanowires by CB[8]-induced host–guest supramolecular interactions and enzyme simulation. The Se-FGG-GST

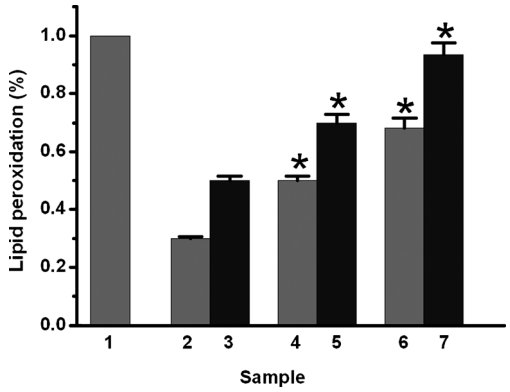

Figure 5. Inhibition of MDA content by Se-FGG-GST (Y6C) nanowires and Se-FGG-GST (Y6C) monomers. Sample 1 is the positive control (100%) in lipid peroxidation, samples 2, 4, and 6 are Se-FGG-GST (Y6C) nanowires. Se-FGG-GST (Y6C) solution concentration in samples 2, 4, and 6 are 50 nM, 25 nM, and 10 nM, respectively; a 1:2 ratio of CB[8] to Se-FGG-GST (Y6C) was used. Solution concentration of Se-FGG-GST (Y6C) monomers in samples 3, 5, and 7 are 50 nM, 25 nM, and 10 nM, respectively.

(Y6C) nanowires exhibited high stability and significant antioxidative properties for protecting mitochondria from oxidative stress, and was shown to be a better antioxidant than Se-FGG-GST (Y6C) monomers. The combination of CB[8]-mediated host–guest interactions with enzyme simulation presents a powerful method for the construction of high-order protein nanostructures. The constructed functional protein nanostructures hold great promise for catalysis, biosensors, and pharmaceuticals.

Received: January 26, 2013
Revised: March 11, 2013
Published online: April 19, 2013

Keywords: cucurbit[8]uril · host-guest systems · nanowires · proteins · self-assembly

[1] a) E. R. Ballister, A. H. Lai, R. N. Zuckermann, Y. Cheng, J. D. Mougous, *Proc. Natl. Acad. Sci. USA* **2008**, *105*, 3733 – 3738; b) T. F. Chou, C. So, B. R. White, J. C. T. Carlson, M. Sarikaya, C. R. Wagner, *ACS Nano* **2008**, *2*, 2519 – 2525; c) E. H. M. Lempens, I. van Baal, J. L. J. van Dongen, T. M. Hackeng, M. Merkx, E. W. Meijer, *Chem. Eur. J.* **2009**, *15*, 8760 – 8767.

[2] a) W. Q. Shen, H. Zhong, D. Neff, M. L. Norton, *J. Am. Chem. Soc.* **2009**, *131*, 6660 – 6661; b) Q. Li, D. Hapka, H. Chen, D. A. Vallera, C. R. Wagner, *Angew. Chem.* **2008**, *120*, 10333 – 10336; *Angew. Chem. Int. Ed.* **2008**, *47*, 10179 – 10182; c) N. Dotan, D. Arad, F. Frolow, A. Freeman, *Angew. Chem.* **1999**, *111*, 2512 – 2515; *Angew. Chem. Int. Ed.* **1999**, *38*, 2363 – 2366.

[3] a) J. Lagona, P. Mukhopadhyay, S. Chakrabarti, L. Isaacs, *Angew. Chem.* **2005**, *117*, 4922 – 4949; *Angew. Chem. Int. Ed.* **2005**, *44*, 4844 – 4870; b) K. Kim, *Chem. Soc. Rev.* **2002**, *31*, 96 – 107; c) J. Zhang, R. J. Coulston, S. T. Jone, J. Geng, O. A. Scherman, C. Abell, *Science* **2012**, *335*, 690 – 694.

[4] a) Y. H. Ko, K. Kim, J. K. Kang, H. Chun, J. W. Lee, S. Sakamoto, K. Yamaguchi, J. C. Fettinger, K. Kim, *J. Am. Chem. Soc.* **2004**, *126*, 1932 – 1933; b) F. Biedermann, E. Elmalem, I. Ghosh, W. M. Nau, O. A. Scherman, *Angew. Chem.* **2012**, *124*, 7859 – 7863; *Angew. Chem. Int. Ed.* **2012**, *51*, 7739 – 7743; c) E. A. Appel, X. J. Loh, S. T. Jones, F. Biedermann, C. A. Dreiss, O. A. Scherman, *J. Am. Chem. Soc.* **2012**, *134*, 11767 – 11773; d) J. Zhang, Y. Liu, B. Yuan, Z. Wang, M. Schönhoff, X. Zhang, *Chem. Eur. J.* **2012**, *18*, 14968 – 14973; e) Y. Liu, K. Liu, Z. Wang, X. Zhang, *Chem. Eur. J.* **2011**, *17*, 9930 – 9935.

[5] a) M. E. Bush, N. D. Bouley, A. R. Urbach, *J. Am. Chem. Soc.* **2005**, *127*, 14511 – 14517; b) H. D. Nguyen, D. T. Dang, J. L. J. van Dongen, L. Brunsveld, *Angew. Chem.* **2010**, *122*, 907 – 910; *Angew. Chem. Int. Ed.* **2010**, *49*, 895 – 898; c) D. T. Dang, J. Schill, L. Brunsveld, *Chem. Sci.* **2012**, *3*, 2679 – 2684.

[6] a) W. Zhang, Q. Luo, L. Miao, C. X. Hou, Y. S. Bai, Z. Y. Dong, J. Y. Xu, J. Q. Liu, *Nanoscale* **2012**, *4*, 5847 – 5851; b) A. E. Salinas, M. G. Wong, *Curr. Med. Chem.* **1999**, *6*, 279 – 309.

[7] a) H. J. Yu, J. Q. Liu, A. Bock, J. Li, G. M. Luo, J. C. Shen, *J. Biol. Chem.* **2005**, *280*, 11930 – 11935; b) C. X. Hou, Q. Luo, J. Q. Liu, L. Miao, C. Q. Zhang, Y. Z. Gao, X. Y. Zhang, J. Y. Xu, Z. Y. Dong, J. Q. Liu, *ACS Nano* **2012**, *6*, 8692 – 8701; c) J. Q. Liu, G. M. Luo, X. J. Ren, Y. Mu, Y. Bai, J. C. Shen, *Biochem. Biophys. Acta* **2000**, *1481*, 222 – 228; d) Z. Y. Dong, Q. Luo, J. Q. Liu, *Chem. Soc. Rev.* **2012**, *41*, 7890 – 7908; e) X. Huang, X. M. Liu, Q. Luo, J. Q. Liu, J. C. Shen, *Chem. Soc. Rev.* **2011**, *40*, 1171 – 1184.

[8] a) H. Sies, *Free Radical Biol. Med.* **1993**, *14*, 313 – 323; b) G. Mugesh, M. Du, W. W. du Mont, H. Sies, *Chem. Rev.* **2001**, *101*, 2125 – 2179.

